Optical Materials 35 (2013) 1418–1421

Contents lists available at SciVerse ScienceDirect

Optical Materials

journal homepage: www.elsevier.com/locate/optmat

Liquid crystal alignment by polyhedral oligomeric silsesquioxane (POSS)–polyimide nanocomposites

Han-Shiang Liu [a], Shie-Chang Jeng [b,*]

[a] Institute of Photonics System, National Chiao Tung University, Tainan 711, Taiwan
[b] Institute of Imaging and Biomedical Photonics, National Chiao Tung University, Tainan 711, Taiwan

ARTICLE INFO

Article history:
Received 19 December 2012
Accepted 18 February 2013
Available online 16 March 2013

Keywords:
Liquid crystal alignment
Nanocomposites
POSS–polyimide
No-bias OCB LCDs

ABSTRACT

Polyimide (PI) films are widely used in the liquid crystal display (LCD) industry to align liquid crystal (LC) molecules in a specific orientation with a pretilt angle θ_p on the PI alignment films. It was observed that physical dispersion of polyhedral oligomeric silsesquioxane (POSS) nanoparticles in commercial homogenous PIs decreases the surface energy of the PI alignment films and generates a controllable θ_p in the range $0° < \theta_p < 90°$, which is not easily achieved by complicate PI synthesis. Characteristics of POSS–PI nanocomposites were studied to investigate the influence of POSS nanoparticles on PIs. Increased absorption in the infrared spectra and decreased decomposition temperature and glass transition temperature with POSS doped concentration in PI were observed due to the increase in free volume of POSS–PI nanocomposites. Such nanoscale hybridization suggests a novel approach to tune the properties of PIs through modification of molecular interaction. A fast response no-bias optically-compensated bend (OCB) LCD with a pretilt angle of 68° was also demonstrated in this work.

1. Introduction

An aromatic polyimide (PI) is a type of high-performance polymeric material characterized by its outstanding mechanical, thermal and electro-optical properties at elevated temperatures, leading to its being widely applied in the electronics and photonics industries. One of the major applications of PIs in the photonics industry is as alignment films for liquid crystal displays (LCDs) to align LC molecules in a certain orientation with a specific pretilt angle θ_p, which is the angle between the LC director and the alignment films. The pretilt angle is very important and required for LC devices to obtain defect-free alignment and also to improve their electro-optical performance, such as driving voltage, response time, color performance and viewing angle. The synthesis of PIs used to produce the homogeneous ($\theta_p \sim 0°$) and homeotropic ($\theta_p \sim 90°$) surface alignments in the LCD industry is a mature technology [1–4]. However, only a small tuning range of pretilt angle is feasible in these commercial PI materials resulting in limited application to LCDs requiring different pretilt angles, such as near zero degrees for in-plane switching LCDs, few degrees for twist-nematic (TN) LCDs, more than 5° for the supertwist-nematic (STN) LCDs, 45–60° for no-bias optically-compensated bend (OCB) LCDs and the bistable bend-splay LCDs and near 90° for the vertically-aligned LCDs. The OCB LCD has been known as a fast LCD mode [5]. It is operated between the bend state and the near homeotropic state at a high voltage. However, the traditional OCB cell with low pretilt angle is actually stable in the splay state. Due to the energy barrier between the splay and bend state of a traditional low pretilt OCB LCD, a holding bias voltage is needed to maintain the OCB LCD in the bend state [6,7]. The no-bias OCB LCD is made possible by using alignment films with sufficiently high pretilt angles to produce an initially stable bend state. Many methods have been developed to control the pretilt angle of LC by using conventional PIs, such as mixing homogenous and homeotropic PIs [8] and stacked PI alignment layers [9].

We have found that the pretilt angle of PIs can be well controlled by adding polyhedral oligomeric silsesquioxane (POSS) nanoparticles to homogenous PIs [10,11]. The addition of the different concentrations of POSS in homogenous PIs generates a variable pretilt angle which can be tuned continuously over the range $0° < \theta_p < 90°$. However, the characteristics of POSS–PI nanocomposite films for LC alignment have not been studied in depth to understand the influence of POSS nanoparticles in PIs. It is interesting to note that several types of nanoparticles have been dispersed in polymer to enhance the thermal, mechanical, electrical and optical properties of polymeric systems through modification of molecular interaction [12–14].

In this work, the Fourier transform infrared (FT-IR) spectra, the decomposition temperature and the glass transition temperature, of POSS–PI nanocomposite films were measured to study the

* Corresponding author. Address: No. 301, Gaofa 3rd Rd., Tainan 711, Taiwan. Tel.: +886 6 303 2121x57830; fax: +886 6 303 2535.
E-mail address: scjeng@faculty.nctu.edu.tw (S.-C. Jeng).

0925-3467/$ - see front matter © 2013 Elsevier B.V. All rights reserved.
http://dx.doi.org/10.1016/j.optmat.2013.02.011

influence of POSS nanoparticles in PIs. The dependence of pretilt angle on surface energy of POSS–PI nanocomposite films was determined. Finally, a fast response no-bias OCB LCD with a pretilt angle ~68° was demonstrated, with a fast response time ~3.4 ms, one order of magnitude faster than conventional TN LCDs.

2. Experimental

Several commercial homogeneous polyamic acids (PAAs) materials from Chimei, Daily Polymer and Nissan Chemical have been tried and worked well for the proposed method. A new fabrication process and a new PAA material were applied in this work for obtaining more repeatable results than previous experiments [10,11]. The PAA (AL-58) purchased from Daily Polymer was used in this work. The solid content of the PAA is ~6 wt%. The POSS nanoparticle, PSS-(3-(2-aminoethyl)amino)propyl-heptaisobutyl substituted POSS (Sigma–Aldrich) as shown in Fig. 1 [15], was purchased and used in the experiment without further treatment and purification. A powerful ultrasonic processor (Misonix S4000) was applied for obtaining a good dispersion of 0.2 wt% POSS doped in PAA. The mixture was then filtered through a 200 nm syringe filter, and then it was diluted with pure PAA in order to generate concentrations of POSS in PAA varying between 0.01% and 0.07% by weight. The POSS–PAA mixture was cast onto indium tin oxide (ITO) conducting glass substrates to obtain a POSS–PI alignment film of ~100 nm in thickness determined by an ellipseometer. The alignment film was first prebaked at 100 °C for 10 min followed by hard baking at 180 °C for 4 h in a vacuum oven to allow imidization of the POSS–PI nanocomposite films.

The spectrometer (Acton SP2150) was used to record the UV–vis spectra of the POSS–PI nanocomposite films. FT-IR spectra of POSS–PI nanocomposite films were recorded by a FT-IR spectrometer (Nicolet Nexus 470) operated at the attenuated total reflectance mode under the protection of nitrogen. The thermal stability of the POSS–PI nanocomposite films was characterized by thermogravimetric analysis (TGA) with a thermogravimetric analyzer (TA Instrument 2050) at a heating rate of 2 °C/min under the protection of nitrogen. The 5% and 10% weight losses temperatures ($T_{d5\%}$,$T_{d10\%}$) and the weight percentage remaining at 600 °C (WR_{600}) were calculated to determine the characteristics of the thermal stability of POSS–PI nanocomposite films. The glass-transition temperatures (T_gs) of the POSS–PI nanocomposite films were determined by differential scanning calorimetry (DSC, TechMax DSC6200) under the protection of nitrogen. The scan rate was 10 °C/min for the T_g measurements. The surface energy of POSS–PI nanocomposite films was calculated using the Owen–Wendt method from the contact angle measurements of water and diiodomethane on the films measured by a contact angle analyzer (Creating Nano Technologies CAM-100) [16]. The surface of the POSS–PI nanocomposite films was mechanically buffed once in each direction with a nylon cloth for assembling the antiparallel LC cells and no-bias OCB LC cells with a cell gap of ~4.8 μm. The LC (E7, $\Delta\varepsilon$ = 14.1, $\varepsilon_\perp$ = 5.) was then injected into the empty LC cells using capillary action. The pretilt angle of the antiparallel LC cells was measured by the heterodyne interferometry, which can determine any pretilt angle [17,18]. The voltage-dependent optical transmission of the LC cell, placed between crossed polarizers, was measured using a 637 nm diode laser, and the applied voltage was a 1-kHz square wave.

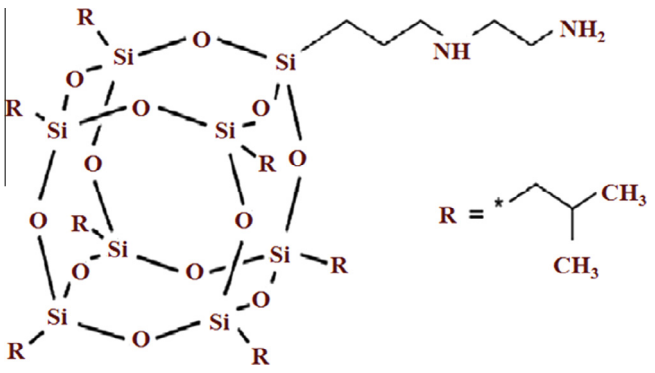

Fig. 1. The structure of polyhedral oligomeric silsesquioxanes (POSS) nanoparticles used in this work [15].

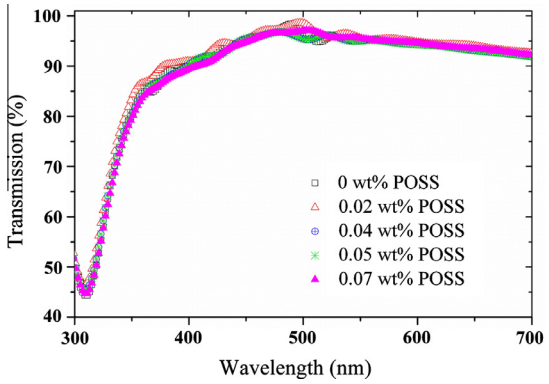

Fig. 2. UV–vis spectra of POSS–PI nanocomposite films with different POSS concentration doped in PAA (film thickness ~550 nm).

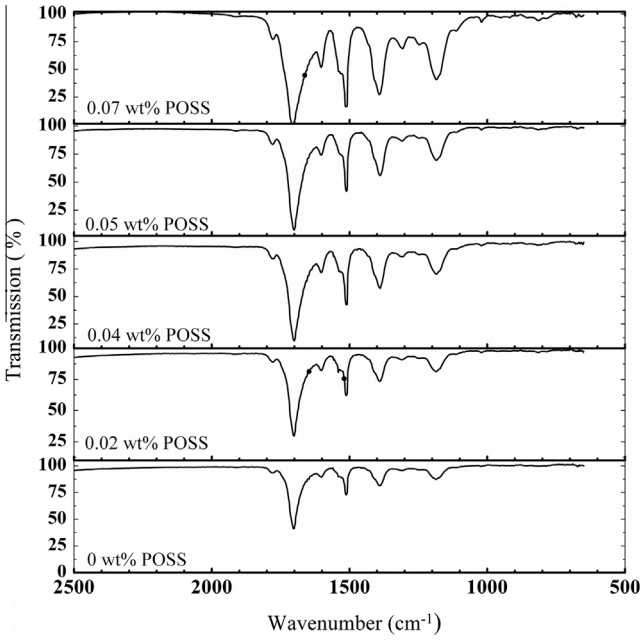

Fig. 3. FT-IR spectra of POSS–PI nanocomposite films with different POSS concentration doped in PAA (film thickness ~550 nm).

3. Results and discussion

The UV–vis absorption spectra of POSS–PI nanocomposite films doped with different POSS concentrations are shown in Fig. 2. It can be seen that the addition of POSS in PIs does not change the absorption properties of POSS–PI nanocomposite films. All POSS–PI nanocomposite films can approach ~90% transmission at wave lengths greater than 400 nm. This lack of color is extremely

Table 1
Imidization of POSS–PI nanocomposite films with different POSS concentration doped in PAA.

POSS concentration in PAA	0 wt%	0.02 wt%	0.04 wt%	0.05 wt%	0.07 wt%
Imidization (%)	89.53	89.68	90.58	92.79	100

Table 2
Thermal properties of POSS–PI nanocomposite films with different POSS concentration doped in PAA.

	$T_{d5\%}$ (°C)[a]	$T_{d10\%}$ (°C)[b]	WR_{600} (wt%)[c]	T_g (°C)[d]
POSS	224	237	35.9	
0 wt% POSS in PAA	299	390	43.4	222
0.02 wt% POSS in PAA	263	322	40.4	221
0.04 wt% POSS in PAA	262	318	37.9	218
0.05 wt% POSS in PAA	261	315	37.2	215
0.07 wt% POSS in PAA	257	300	31.1	213

[a] Thermal decomposition temperature at 5% weight loss.
[b] Thermal decomposition temperature at 10% weight loss.
[c] Weight percentage remaining at 600 °C.
[d] Glass transition temperature.

important for the application of PIs in photonics devices such as LCDs.

The FT-IR spectra of POSS–PI nanocomposite films prepared at different POSS concentration doped in PAA are shown in Fig. 3. The main peaks are the imide carbonyl C=O stretching vibration at ~1704 cm^{-1}, aromatic ring stretching vibration at ~1511 cm^{-1}, imide ring C—N stretching vibration at ~1386 cm^{-1}, and aromatic ether C—O stretching vibration at ~1180 cm^{-1}. The peak from Si—O—Si of POSS at ~1110 cm^{-1} is also visible for PAA doped with 0.07 wt% POSS. It can be observed that the absorption intensities of the characteristic peaks gradually increase with POSS concentration doped in PAA. IR absorption bands are commonly used to determine the amount of imidization of PI [19]. The POSS–PI nanocomposite films were thermally cured at 180 °C for 4 h for PAA converting to PI in this work. The adsorption band at 1386 cm^{-1} (polyimide: C—N stretching vibration) was monitored as an indicator of imidization. The adsorption band at 1511 cm^{-1} is selected as an internal standard. The imidization of PAA to PI for different POSS–PI nanocomposites normalized by 0.07 wt% POSS–PI nanocomposites is determined by the following equation [19]:

$$\text{Imidization}\ (\%) = (D_{1386\ cm^{-1}}/D_{1511\ cm^{-1}})/(D_{1386\ cm^{-1}}/D_{1511\ cm^{-1}})_{0.07\ wt\%} \times 100$$

where D is the optical density.

The imidization of POSS–PI nanocomposite films increases with POSS concentration doped in PAA as shown in Table 1. The increased absorption in the IR spectra and the increase in imidization with POSS concentration doped in PAA are believed due to the increase in free volume of POSS–PI nanocomposite [12–14], which phenomenon is also observed in the later experiments and will be discussed later.

The thermal decomposition temperature at 5% and 10% weight losses, $T_{d5\%}$ and $T_{d10\%}$, respectively, and the weight percentage remaining at 600 °C (WR_{600}) are listed in Table 2. The decomposition temperature $T_{d5\%}$ and $T_{d10\%}$ of POSS–PI nanocomposite films decreases with POSS concentration doped in PAAs due to reduced degradation temperature of POSS ($T_{d5\%} \sim 224$ °C, $T_{d10\%} \sim 237$ °C). The lower thermal stability of POSS also leads to decreased WR_{600} as the concentration of POSS doped in PAAs is increased.

The T_gs of the POSS–PI nanocomposite films are also summarized in Table 2. The T_gs of the POSS–PI nanocomposites are in the range of 213–221 °C, which are slightly lower than pure PI (~222 °C). The T_gs of POSS–PI nanocomposites decrease with the concentration of POSS doped in PAA. The reduction in the dielectric constant, modulus and T_g of PI doped with POSS was observed in previous literatures and it has been interpreted in terms of producing porous silsesquioxane cores of the POSS and the increase of free volume by the presence of POSS structure resulting in a loose PI network [13.14]. The existence of the intermolecular interaction of polyimide segments and tethered POSS could result in a loose PI structure, which induces a stronger absorption in the IR spectra and the increase in imidization as shown in Fig. 3 and Table 1. Due to the increase of free volume, our results of density measurements showed that the density of POSS–PI nanocomposite decreased from 1.55 g/cm^3 to 1.25 g/cm^3 for PAA doped with 0.1 wt% POSS.

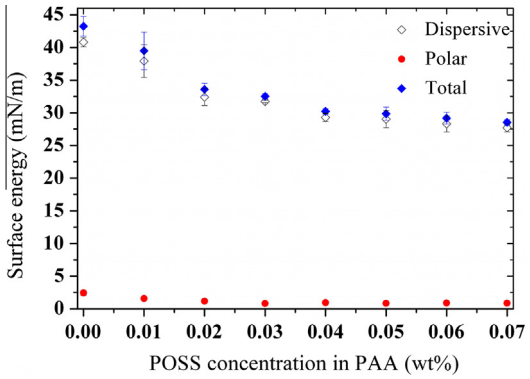

Fig. 4. Total surface energy, polar surface energy and dispersion surface energy as functions of POSS concentration doped in PAA.

The surface energy, including polar and dispersive, of POSS–PI nanocomposite films determined by contact angle measurement is shown in Fig. 4. The addition of POSS in PI decreases the surface energy with POSS concentration doped in PAA. Fig. 5 shows the pretilt angle of POSS–PI nanocomposite films as a function of concentration of POSS doped in PAA. A wide range of pretilt angle from ~0° to ~90° can be generated by varying the POSS concentration from 0 wt% to 0.07 wt%. The concentration of POSS used here was lower than our previous work due to the difference in PAA material and dispersion processes [10]. The reduction of POSS nanoparticles doped in PI can reduce the scattering of POSS–PI alignment films from aggregation of POSS nanoparticles. The LC alignment on POSS–PI nanocomposite films can be explained by the empirical Friedel–Creagh–Kmetz (FCK) rule [20]. The FCK rule indicates that the pretilt angle depends on the surface energy of the alignment film. An alignment film with a higher surface energy favors a lower pretilt angle and vice versa. The pretilt angle of the LC on a PI alignment surface is determined by several factors, such as anchoring, steric effect, electronic interaction, and surface energy [21]. The influence of surface polarity of alignment films on pretilt angle has been investigated [21–23]. The results showed that an alignment film with larger polar surfaces provides a lower pretilt angle due to the increased attractive interaction between LC and the alignment surface.

One fast response no-bias OCB LCD was demonstrated using POSS–PI nanocomposites as the alignment films in this work. One traditional OCB LCD without POSS doped in PAA ($\theta_p \sim 2°$) and one proposed no-bias OCB LCD with 0.05 wt% POSS doped in

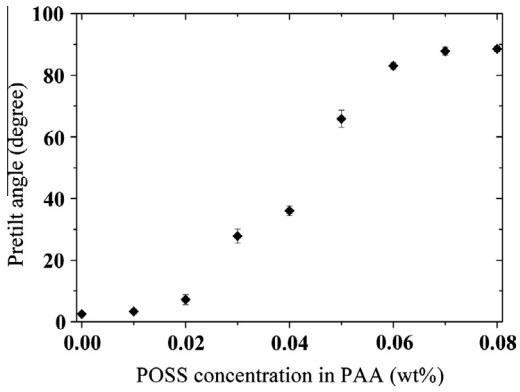

Fig. 5. Dependence of pretilt angle on POSS concentration doped in PAA.

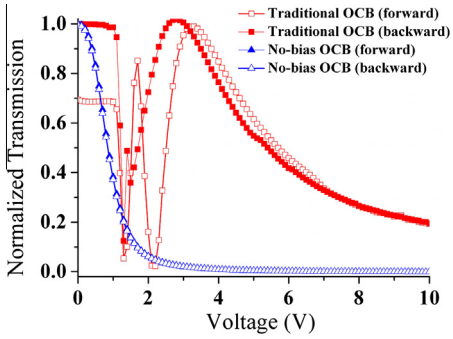

Fig. 6. Voltage dependent transmission curves of the traditional and no-bias OCB LCDs by applying forward (0–10 V) and backward (10–0 V) voltages.

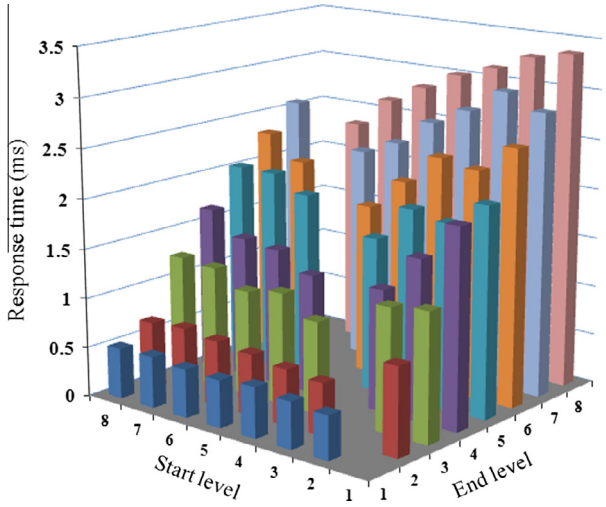

Fig. 7. The response times for switching between gray levels for the no-bias OCB LCD.

PAA ($\theta_p \sim 68°$) were fabricated for comparison. Voltage dependent transmission properties are shown in Fig. 6, obtained by applying forward voltage (0–10 V) and backward voltage (10–0 V) and recording data for one second at the first second after the voltage was applied. Here, the curves are normalized to the maximum transmission. The pretilt angle of the no-bias OCB LCD with 0.05 wt% POSS doped in PAA is 68° larger than the critical angle of ~48° [6,7]. Therefore, the proposed no-bias OCB LCD could overcome the energy barrier and maintain an initially stable bend state. As shown in Fig. 6, the two curves of no-bias OCB LCD obtained by applying forward and backward voltages overlap very well because no transient time is required to transform between the two states as in a traditional low pretilt OCB LCD. The response times, rise time t_r and fall time t_f, for switching between various gray levels for the no-bias OCB LCD are shown in Fig. 7. The eight gray levels are defined as evenly spaced transmission states with one representing the dark state and eight representing the maximum transmission. We found that the switching time between most gray levels is less than 3 ms, and the average total response time, $t_r + t_f$, is around ~3.4 ms, one order of magnitude faster than the conventional TN LCDs.

4. Conclusions

This work has applied POSS nanoparticles doped in commercial homogeneous PI. The physical dispersion of POSS in PIs lowers T_d and T_g, and enhances the imidizaion of POSS–PI nanocomposite films due to the increase of the free volume with the POSS concentration doped in PIs. The proposed POSS–PI nanocomposite films can be applied in LCDs for generating controllable pretilt angle from $0° < \theta_p < 90°$ by modification of the surface energy of PIs through the addition of POSS. A fast-response no-bias OCB LCD was demonstrated using POSS–PI nanocomposites alignment films. The proposed method is fully compatible with current manufacture processes of LCD industry.

Acknowledgements

The authors would like to thank the National Science Council of Taiwan for financially supporting this research under Contract: NSC 100-2112-M-009 -014 -MY3. The authors are grateful to Dr. Huai-Pin Hsueh from Chimei for supporting PI materials and helpful discussions.

References

[1] M. Nishikawa, Polym. Adv. Technol. 11 (2000) 404.
[2] J.H. Park, J.C. Jung, B.-H. Sohn, S.W. Lee, M. Ree, J. Polym. Sci. Part A: Polym. Chem. 39 (2001) 3622.
[3] N.V. Kamanina, Features of Liquid Crystal Display Materials and Processes, InTech, Rijeka, Croatia, 2011.
[4] Y.J. Lee, J.G. Choi, I.K. Song, J.M. Oh, M.H. Yi, Polymer 47 (2006) 1555.
[5] E.J. Acosta, M.J. Towler, H.G. Walton, Liq. Cryst. 27 (2000) 977.
[6] F.S. Yeung, H.S. Kwok, Appl. Phys. Lett. 88 (2006) 063505.
[7] J.B. Kim, K.C. Kim, H.J. Ahn, B.H. Hwang, J.T. Kim, Appl. Phys. Lett. 91 (2007) 023507.
[8] F.S. Yeung, J.Y. Ho, Y.W. Li, F.C. Xie, O.K. Tsui, P. Sheng, H.S. Kwok, Appl. Phys. Lett. 88 (2006) 051910.
[9] Y.J. Lee, J.S. Gwag, Y.K. Lim, S.I. Jo, S.G. Kang, Y.R. Park, J.H. Kim, Appl. Phys. Lett. 94 (2009) 041113.
[10] S.-J. Hwang, S.-C. Jeng, I.-M. Hsieh, Opt. Express. 18 (2010) 16507.
[11] S.-C. Jeng, S.-J. Hwang, T.-A. Chen, H.-S. Liu, M.-Z. Chen, Proc. SPIE 3768 (1999) 462.
[12] T.C. Merkel, B.D. Freeman, R.J. Spontak, Z. He, I. Pinnau, P. Meakin, A.J. Hill, Science 296 (2002) 519.
[13] C.M. Leu, Y.T. Chang, K.H. Wei, Chem. Mater. 15 (2003) 3721.
[14] Y.J. Lee, J.M. Huang, S.W. Kuo, J.S. Lu, F.C. Chang, Polymer 46 (2005) 173.
[15] Sigma–Aldrich. <https://www.sigmaaldrich.com/>
[16] D.K. Owens, R. Wendt, J. Appl. Polym. Sci. 13 (1969) 1741.
[17] S.J. Hwang, M.H. Hsu, J. Soc. Inf. Display 14 (2006) 1039.
[18] K.H. Chen, W.Y. Chang, J.H. Chen, Opt. Express 17 (2009) 14143.
[19] C.A. Pryde, J. Polym. Sci. Part A: Polym. Chem. 27 (1989) 711.
[20] J. Cognard, Mol. Cryst. Liq. Cryst. Suppl. Ser. A5 (1982) 1.
[21] S.H. Paek, C.J. Durning, K.W. Lee, A. Lien, J. Appl. Phys. 83 (1998) 1270.
[22] B.S. Ban, Y.B. Kim, J. Appl. Polym. Sci. 74 (1999) 267.
[23] H.Y. Wu, C.Y. Wang, C.J. Lin, R.P. Pan, S.S. Lin, C.D. Lee, C.S. Kou, J. Phys. D 42 (2009) 155303.